AIP Journal of Applied Physics

Anisotropic electromagnetic properties of polymer composites containing oriented multiwall carbon nanotubes in respect to terahertz polarizer applications

D. S. Bychanok, M. V. Shuba, P. P. Kuzhir, S. A. Maksimenko, V. V. Kubarev et al.

Citation: J. Appl. Phys. **114**, 114304 (2013); doi: 10.1063/1.4821773
View online: http://dx.doi.org/10.1063/1.4821773
View Table of Contents: http://jap.aip.org/resource/1/JAPIAU/v114/i11
Published by the AIP Publishing LLC.

JOURNAL OF APPLIED PHYSICS **114**, 114304 (2013)

Anisotropic electromagnetic properties of polymer composites containing oriented multiwall carbon nanotubes in respect to terahertz polarizer applications

D. S. Bychanok,[1,a)] M. V. Shuba,[1] P. P. Kuzhir,[1] S. A. Maksimenko,[1] V. V. Kubarev,[2] M. A. Kanygin,[3] O. V. Sedelnikova,[3] L. G. Bulusheva,[3] and A. V. Okotrub[3]

[1]*Research Institute for Nuclear Problems, Belarusian State University, 11 Bobruiskaya str., 220030 Minsk, Belarus*
[2]*Budker Institute of Nuclear Physics, SB RAS, 11 Acad. Lavrentiev av., 630090 Novosibirsk, Russia*
[3]*Nikolaev Institute of Inorganic Chemistry, SB RAS, 3 Acad. Lavrentiev av., 630090 Novosibirsk, Russia*

(Received 21 June 2013; accepted 3 September 2013; published online 17 September 2013)

Polystyrene composites with 0.5 wt. % loading of oriented multiwall carbon nanotubes (MWCNTs) have been produced by forge rolling method. The composites showed anisotropy of transmission and reflection of terahertz radiation depending on sample orientation relative to the polarization of electromagnetic wave. The structural characteristics of composites (nanotube ordering, length, defectiveness) were estimated by fitting the theoretical dependencies calculated within the Clausius-Mossotti formalism for cylindrical particles to the experimental data. The presented model was used for prediction of electromagnetic response of composites containing oriented MWCNTs with various structural parameters in THz region.
[http://dx.doi.org/10.1063/1.4821773]

I. INTRODUCTION

Interest in terahertz radiation is provoked by the development and production of tomography and scanning quality control equipment, radio astronomy, security systems, etc. Carbon nanotubes (CNTs) owing to peculiar electromagnetic response in this range[1–3] are attractive for such kind of applications. Particularly, the surface plasmon resonance (antenna resonance) inherent in isolated CNT was shown to provide non-Drude conductivity of CNT composites.[4–7] The theoretical description of antenna effect in CNTs in the terahertz range was presented in Refs. 8–11. CNT-based composite materials with tuned electromagnetic response offer many promising opportunities for the terahertz radiation control and manipulation. Actually, the recent progress in investigation of properties of aligned CNT-arrays for optoelectronic applications allowed producing effective terahertz polarizers.[3,12,13] The similar properties of polymer composites, containing aligned CNTs, were also observed in microwave range.[14]

Unique properties of CNTs are provided by the cylindrical structure, high conductivity, and large aspect ratio, causing the anisotropic electromagnetic response of isolated nanotube.[15] It is well known that a little inclusion of CNTs in composite can strongly modify its electromagnetic parameters.[16–20] In the case of polymer composites, the effective permittivity depends on the permittivity of host polymer matrix ε_h and polarizability, concentration, and orientation of inclusions. Variation in these parameters allows tuning the effective permittivity of composite material in wide frequency range. However, analysis of microstructure of CNT-based polymer composites is still a challenging task due to the rigid restriction on the sample thickness for microscopic investigation, melting of polymer under the electron beam, etc. Therefore, today dielectric spectroscopy and theoretical approaches developed for modeling of experimental data are commonly used for characterization of dispersion and geometry of CNTs in polymer matrix.

In present work we studied anisotropy of electromagnetic response of CNT-based polymer composite in terahertz range experimentally and theoretically. The dispersion and alignment of multiwall CNTs (MWCNTs) in polystyrene matrix were achieved by the forge rolling method. The permittivity of composites was simulated using the modified Clausius-Mossotti model. From matching between calculation and experimental data the key structural parameters of MWCNT-composite were determined. Effect of defectiveness and length of nanotubes on the electromagnetic properties of polymer composites was discussed.

II. MATERIALS AND METHODS

A. Carbon nanotube synthesis

Vertically aligned MWCNT arrays were grown on silicon substrates using an aerosol-assisted catalytic chemical vapor deposition (CCVD) method described elsewhere.[21] The solution of ferrocene (2 wt. %) in toluene was injected during 15 min in horizontal tubular reactor heated up to 800 °C.

The structure of obtained samples was characterized by scanning electron microscopy (SEM) on a JEOL JSM-6700 F microscope and transmission electron microscopy (TEM) on a JEOL JEM-2010 microscope. SEM micrographs showed that nanotubes have predominant orientation perpendicularly to silicon substrate (Fig. 1(a)). The height of MWCNT arrays was ~75 μm. The average outer diameter of MWCNTs was estimated from TEM images to be ~30 nm (Fig. 1(b)). Concentration of iron nanoparticles in the MWCNT channels determined by elemental analysis was ~5 wt.%.

[a)]Electronic mail: dzmitrybychanok@ya.ru. URL: www.nano.bsu.by.

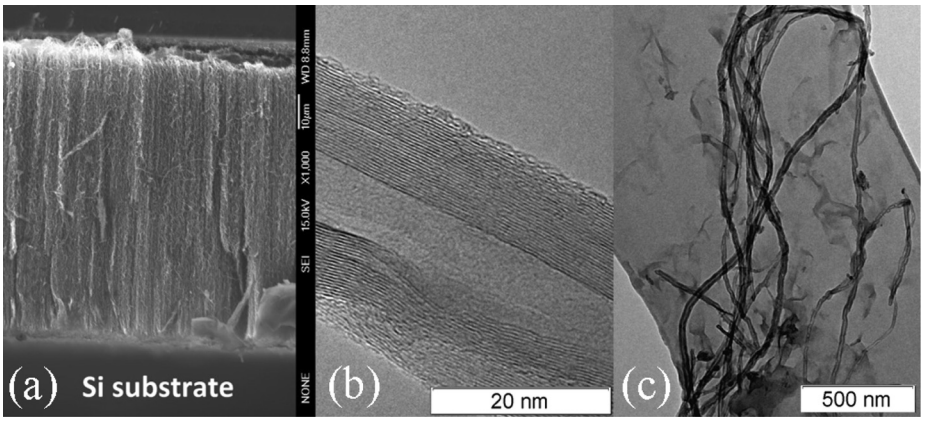

FIG. 1. (a) SEM and (b) TEM images of MWCNTs used for composite preparation, (c) TEM image of MWCNTs extracted from composite by polystyrene dissolving.

B. Composite preparation

Polystyrene composites with the MWCNT loading of 0.5 wt. % were prepared by forge rolling method. Previously, the procedure had been developed for dispersion of onion-like carbon (OLC) nanoparticles in polystyrene matrix.[22] MWCNTs were gently detached from silicon substrates and dispersed in toluene by mechanical stirring for an hour. Polystyrene, taken in the required proportion, was added in the MWCNT-toluene dispersion, and the obtained mixture was stirred until complete dissolution of polymer, followed by ultrasonication treatment for 5 min (200 W/10 ml) and stirring for 2 h. Obtained composite slush was applied over aluminium foil plate and dried at ambient conditions during 3 h to the viscous state. Then the sample was repeatedly forge-rolled in certain direction until the composite got a uniform gray color. The obtained plate with a thickness of $\sim$360 μm was dried under a light load at room temperature during 12 h. We suggest that saving the forge rolling direction would result in predominant orientation of MWCNTs in polymer matrix.

Disaggregation of MWCNT bundles and their uniform distribution in polystyrene were evidenced from darkening of composite plate after 50 cycles of forge-rolling. Furthermore, fine separation of nanotubes in the matrix was confirmed by TEM examination of sediment, extracted from composite after polystyrene dissolving by toluene (Fig. 1(c)). A typical image shows that sediment contains isolated nanotubes coated by polystyrene mantle. Also, our previous investigations[23] showed that strong forces of the rolls could break the nanotubes and lead to decreasing of average nanotube length in composite.

C. Measurement details

The samples with lateral dimensions $20 \times 30\,\mathrm{mm}^2$ were taken for measurements. The resistivity of composite plates measured by two-contact method showed a value of $\sim 10^{10}\,\Omega$ that allows concluding that MWCNTs in polystyrene matrix are isolated from each other.

Transmission and reflection spectra of the plates were recorded in a range of 0.5–3.5 THz using a Bruker IFS 66vs vacuum Fourier spectrometer with liquid helium-cooled bolometer. The linear polarized beam had normal incidence for transmission and 85° incidence for reflection. The composite sample was rotated in azimuth plane so that the electric field was parallel ($T_\parallel$ and $R_\parallel$) or perpendicular ($T_\perp$ and $R_\perp$) to the forge rolling direction. Diameter of incident beam was $\sim$12 mm.

D. Simulation details

The permittivity tensor of composite material, consisting of polymer matrix and isolated MWCNTs, can be calculated using the Clausius-Mossotti model, modified for cylindrical inclusions[24]

$$\hat{\varepsilon} = \hat{I}\left[1 + \frac{N_h\alpha_h/\varepsilon_0}{1 - N_h\alpha_h/(3\varepsilon_0)}\right] + \int_0^\pi\int_0^\pi \psi(\theta,\varphi)\frac{N\alpha_\parallel\hat{T}/\varepsilon_0}{1 - Nn_\parallel\alpha_\parallel/\varepsilon_0}\sin\theta d\theta d\varphi, \quad (1)$$

where $\hat{I}$ is the unit matrix, $\varepsilon_0 = 8.85 \times 10^{-12}\,\mathrm{Fm}^{-1}$ is the vacuum permittivity, N_h and N are the numbers of host matrix molecules and MWCNTs in volume unit, α_h is the polarizability of host matrix molecules, $\alpha_\parallel$ is the axial polarizability of MWCNT (we assume that axial polarizability is much bigger that the transverse one), $\psi(\theta,\varphi)$ is the orientation dispersion function of inclusions in composite, and $\hat{T} = \tilde{A} \otimes A$ is the tensor product of two projection vectors $A = (\sin\theta\cos\varphi, \sin\theta\sin\varphi, \cos\theta)$. The longitudinal depolarization factor of cylinder $n_\parallel$ is described as[25]

$$n_\parallel = \frac{6r^2}{l^2}\left[\ln\left(\frac{2l}{r}\right) - \frac{7}{3}\right], \quad (2)$$

where r is the cylinder radius and l is the cylinder length ($l \gg r$).

According to Ref. 14, the orientation dispersion function $\psi(\theta,\varphi)$ can be found by the following equation:

$$\psi(\theta,\varphi) = \frac{\chi^2}{2\pi[\chi^2\cos^2\theta + \sin^2\theta(\chi^2\cos^2\varphi + \sin^2\varphi)]^{3/2}}, \quad (3)$$

where parameter $\chi \geq 1$ characterizes predominant ordering of MWCNTs along the rolling direction. Rolling direction $(\theta,\varphi) = (\pi/2, \pi/2)$ corresponds to oY-direction in the

Cartesian coordinate system. In this case the components of dielectric permittivity tensor may be transformed as $\varepsilon_{yy} = \varepsilon_{\parallel}$ and $\varepsilon_{xx} = \varepsilon_{zz} = \varepsilon_{\perp}$.

For calculation of the $\alpha_{\parallel}$ value a theoretical model[26] has been used, where MWCNT is considered as finite-length multishell structure consisting of coaxial, infinitely thin conductive cylinders. The conductivity σ_i of each shell was considered by the following equation:[1]

$$\sigma_j = -\frac{ie^2}{\pi^2\hbar R(\omega + i\nu)} \sum_{s=1}^{m} \int_{1stBZ} \frac{\partial F_c}{\partial p_z}\frac{\partial E_s}{\partial p_z} dp_z, \tag{4}$$

where $\hbar$ is the normalized Planck constant, e is the electron charge, and p_z is the axial projection of quasimomentum. The integer $s = 1, 2, 3...m$ labels the π-electron energy bands E_s, m is an index appearing in the dual indexes (m, n) used to classify CNT, ω and ν are the angular and relaxation frequencies. The abbreviation $1stBZ$ restricts the variable p_z to the first Brillouin zone, and F_c is the equilibrium Fermi distribution function.

The total axial conductivity of MWCNT σ was calculated from the Maxwell equations with effective boundary conditions for the electromagnetic field on the MWCNT surface using Eq. (4) for each shell (see details in Ref. 26). Than the axial polarizability of MWCNT was obtained from conductivity using a simple relation

$$\alpha_{\parallel} = \frac{i\sigma}{\omega}. \tag{5}$$

The electromagnetic response of the MWCNT-based composite was calculated via the Fresnel formulas using the polarizability of nanotubes calculated by the Eq. (5). To apply the model presented above for description of the experimentally measured electromagnetic response of MWCNT-polystyrene composites, we fixed the permittivity of matrix ($\varepsilon_h = 2.5$, this is typical value for permittivity of polystyrene in THz region[27]), radius, and concentration of MWCNTs ($r = 15$ nm and $n = 0.5$ wt. %) and thickness of composite plate ($d = 360\,\mu$m). Thus, the most important variables, which impact on electromagnetic response of composite, are the MWCNTs ordering state, their length l, and defectiveness. The first variable is determined by the parameter χ (Eq. (3)), and the latter one is influenced by the relaxation time τ.

III. EXPERIMENTAL AND SIMULATION RESULTS

A. Experimental data and comparison with numerical results

The frequency dependencies of experimentally measured electromagnetic response of polystyrene composite are presented in Fig. 2. From the transmission spectra (solid symbols) one can see that even relatively small addition of MWCNTs in polystyrene matrix provides noticeable attenuation of electromagnetic radiation in the THz frequency range (Fig. 2(a)). The reflection (open symbols) has an oscillator-like dependence (Fig. 2(b)), which indicates the Fresnel reflection from the samples surfaces. However, for both polarizations, the average values of reflection remain rather low, so the recession of the transmission is mainly caused by frequency dependence of MWCNT polarizability, which will be discussed below.

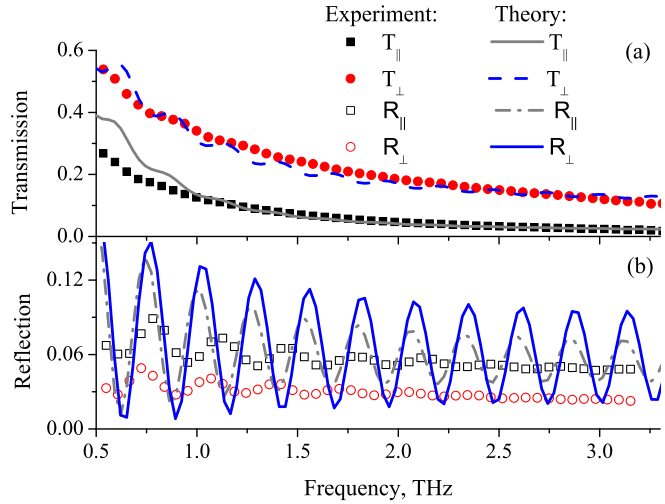

FIG. 2. Results of experimental measurements and theoretical modeling of polystyrene composite with 0.5 wt. % MWCNTs loading: (a) transmission T and (b) reflection R spectra for parallel ($E \parallel$ MWCNTs) and perpendicular ($E\perp$ MWCNTs) orientation of sample relative to polarization of incident wave. The fitting parameters: $l = 1.2\,\mu$m, $r = 15$ nm, $\tau = 2$ fs, $n = 0.5$ wt.%, $\varepsilon_h = 2.5$, $d = 360\,\mu$m.

Transmission and reflection of the composite are strongly dependent on orientation of the plate in respect to the polarization of electromagnetic wave. Hence, the forge rolling procedure causes alignment of MWCNTs in polystyrene matrix, thus producing a composite with anisotropic properties. The transmission $T_{\perp}$ decreases from 0.54 to 0.10 in the frequency interval from 0.5 to 3.5 THz. The reflection $R_{\perp}$ is ~0.03. For parallel orientation of the electric field vector, MWCNTs absorb and reflect the incident radiation stronger. Indeed, near 0.5 THz the transmission $T_{\parallel}$ is about two times smaller than the corresponding value of $T_{\perp}$, and starting from 2 THz the composite is almost opaque to the electric field being parallel to the rolling axis ($0.04 < T_{\parallel} < 0.02$ in 2.0–3.5 THz frequency range). The reflection $R_{\parallel}$ decreases from 0.09 to 0.05 between the 0.5–3.5 THz frequencies.

The theoretical best fits to the experimental data are shown in Fig. 2 by solid and dashed lines. The chosen parameters required for the model described in Sec. II D are $\chi = 1.7$, $l = 1.2\,\mu$m, and $\tau = 2$ fs. Note that nanotube length used for the theoretical calculations is significantly less than the length of initial MWCNTs inserted in polystyrene because of hard forces developed during the forge rolling procedure resulting in fracture of MWCNTs. Previously, the partial breaking of OLC agglomerates and MWCNTs has been deduced from the electromagnetic examination of polymer composites prepared by this method.[22,23,28] Statistical analysis of the TEM images of MWCNTs dispersed in polystyrene confirmed the nanotube shortening up to about 0.5–2.5 μm in the result of the forge rolling.[29]

The good agreement between theory and experiment (Fig. 2) demonstrates the capability of the used model for prediction of the exact geometry of composite material,

which could provide electromagnetic response necessary for practical applications. In particular, with the same content of MWCNTs in the matrix, the properties of the composite will be different depending on the orientation of the individual filler particles, their length and defectiveness. Effect of these key structural parameters (χ, l, and τ) on the electromagnetic response of composite is examined in following Subsections III B-III D.

B. Orientation dependence

Let us fix parameters of MWCNTs (i.e., $r = 15$ nm, $l = 1.2\,\mu$m, and $\tau = 2$ fs) and consider the influence of nanotube orientation on permittivity of composite ($\varepsilon_h = 2.5$ and $n = 0.5$ wt. %).

Orientation dispersion of MWCNTs in host matrix is described by Eq. (3). The case $\chi = 1$ corresponds to randomly oriented inclusions, so composite material is macroscopically isotropic. The orientation dispersion function $\psi(\theta, \varphi) = 1/2\pi$ and the permittivity tensor $\hat{\varepsilon}$ becomes scalar

$$\varepsilon_u = 1 + \frac{N_h\alpha_h/\varepsilon_0}{1 - N_h\alpha_h/(3\varepsilon_0)} + \frac{1}{3}\frac{N\alpha_\parallel/\varepsilon_0}{1 - Nn_\parallel\alpha_\parallel/\varepsilon_0}. \quad (6)$$

Parameter $\chi \geq 1$ corresponds to predominant ordering of MWCNT along a certain direction. For the samples investigated here $\chi = 1.7$, which indicates alignment of nanotubes along the forge rolling direction oY. The real and imaginary parts of components $\varepsilon_\parallel$ and $\varepsilon_\perp$ are presented in Fig. 3(a) together with those calculated for ε_u, which correspond to composite contained the same concentration of randomly distributed MWCNTs. As compared to ε_u dependences, both parts are larger for the component $\varepsilon_\parallel$ and smaller for $\varepsilon_\perp$ one. This is in good correspondence with our previous results obtained for the microwave frequency range.[14]

Irrespective of MWCNT orientation, the $Im(\varepsilon)$ dependence has maximum located around 1 THz. This feature is also evident in the frequency dependence of the imaginary part of polarizability of isolated MWCNT (Fig. 3(b)), and it can be

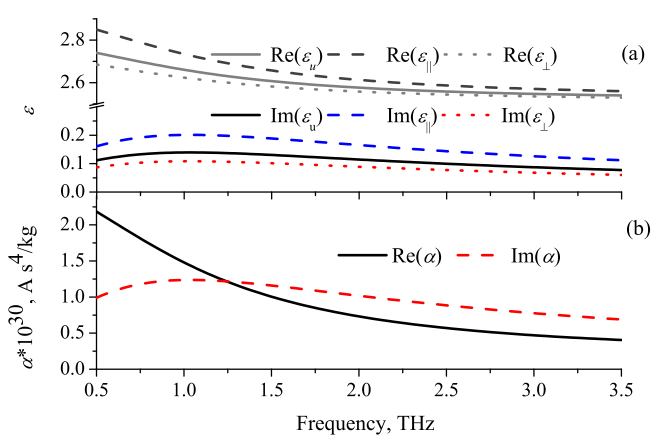

FIG. 3. (a) Frequency dependence of components $\varepsilon_\parallel$ and $\varepsilon_\perp$ of dielectric permittivity tensor for experimentally measured MWCNT-based composite ($\chi = 1.7$) and scalar dielectric permittivity ε_u of composite containing randomly oriented MWCNTs ($\chi = 1$) with the same length, radius, and concentration. (b) Frequency dependence of axial polarizability of MWCNT. The fitting parameters: $l = 1.2\,\mu$m, $r = 15$ nm, $\tau = 2$ fs, $n = 0.5$ wt.%, $\varepsilon_h = 2.5$.

associated with finite length effects described in Ref. 26. Bellow we will show that the maximum position is strongly dependent on nanotube length l and relaxation time τ.

The case when $\chi \to \infty$ is ideal, all inclusions are precisely oriented in the same direction. The components $\varepsilon_\parallel$ and $\varepsilon_\perp$ of permittivity are given by

$$\lim_{\chi\to\infty} \varepsilon_\perp = 1 + \frac{N_h\alpha_h/\varepsilon_0}{1 - N_h\alpha_h/(3\varepsilon_0)} \approx \varepsilon_h, \quad (7)$$

$$\lim_{\chi\to\infty} \varepsilon_\parallel = 1 + \frac{N_h\alpha_h/\varepsilon_0}{1 - N_h\alpha_h/(3\varepsilon_0)} + \frac{N\alpha_\parallel/\varepsilon_0}{1 - Nn_\parallel\alpha_\parallel/\varepsilon_0}. \quad (8)$$

This implies that when all MWCNTs in composite are oriented along one direction, dielectric permittivity in this direction has the form (8). If the electric field polarization $\vec{E}$ of incident electromagnetic wave is perpendicular to this direction, electromagnetic response of composite will be close to response of the host matrix. Therefore anisotropic MWCNT-based composite films are promising for the THz-polarizer applications.

In Secs. III C and III D we will use for calculations the parameter $\chi = 1.7$, which allows matching the theoretical data as closely as possible to the experimental ones (see Sec. III A).

C. Relaxation time dependence

Atomic-scale defects in the MWCNT walls can cause significant scattering of charge carriers and lead to the finite value of relaxation time. The good agreement between the experimental and modeled electromagnetic response of MWCNT-polystyrene composites was obtained for $\tau = 2$ fs. This value is several times smaller than those characteristic of graphite and ideal nanotubes.[26] Variation in relaxation time, i.e., variation in MWCNT defectiveness, permits to find possible ways to tune properties of anisotropic materials. To ascertain how the electron relaxation time affects the electromagnetic response of anisotropic composite we varied this parameter in the range from 0.5 up to 8 fs preserving the other two variables $l = 1.2\,\mu$m and $\chi = 1.7$. The frequency dependencies of axial polarizability of MWCNT and corresponding component $\varepsilon_\parallel$ of MWCNT-based composite for various relaxation times are shown in Figs. 4(a) and 4(b). Since for calculation of permittivity of composite with low concentration of inclusions we used the linear Clausius-Mossotti model, the frequency dependencies of MWCNT polarizability and composite permittivity have the same form and differ from each other by only a scalar factor (see left scale for α and right scale for $\varepsilon_\parallel$ in Fig. 4). Increase of the relaxation time leads to the growth of both real and imaginary parts of polarizability at high frequencies and the shift of the peak of imaginary part to high frequency region. We associate this peak with finite length effects described in Ref. 26.

The obtained frequency dependencies of component $\varepsilon_\parallel$ were used for calculation of the reflection R and transmission T of composite by the Fresnel formulas. The dependencies for different relaxation times are presented in Fig. 5. One can see that increase in relaxation time results in significant

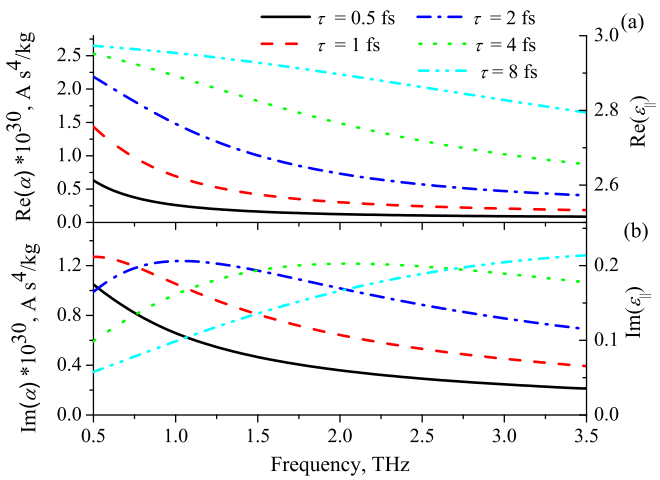

FIG. 4. Frequency dependence of real (a) and imaginary (b) parts of axial polarizability of MWCNT (left scale) and real (a) and imaginary (b) parts of permittivity $\varepsilon_{\parallel}$ of MWCNT-based composite (right scale) for various relaxation times. The fitting parameters: $\chi = 1.7$, $l = 1.2\,\mu$m, $r = 15$ nm, $n = 0.5$ wt.%, $\varepsilon_h = 2.5$.

decrease of transmission at high frequencies (Fig. 5(a)) and also reduce of amplitude of reflection oscillations (Fig. 5(b)). Thus we can conclude that although MWCNTs with the largest relaxation time (i.e., MWCNTs with smallest amount of defects) are most suitable for the THz-polarizer applications, defective MWCNTs (with $\tau \geq 2$ fs) also may be used for production of effective THz shielding and absorbing composites.

Note that defectiveness of nanotubes could be changed by post-processing treatment such as high-temperature annealing. Hereinafter our efforts will be focused on the experimental verification of EM response dependences of CNT-based composites on the defectiveness of the tubes.

D. Length dependence

Frequency dependencies of axial polarizability of MWCNT ($\chi = 1.7$ and $\tau = 2$ fs) and corresponding component $\varepsilon_{\parallel}$ of composites containing MWCNTs of 0.5, 1.2, 2.0, 4.0, and 8 microns length are presented in Figs. 6(a)–6(d). Since the MWCNTs diameter was fixed the change in MWCNTs length from 0.5 to 8 μm corresponds to the variation in aspect ratio from 16 to 270. Here, in contrast to Fig. 4, this change at constant MWCNT concentration n leads to variation in number of nanotubes N in volume unit of composite (see Eq. (1)). As the result the behavior of component $\varepsilon_{\parallel}$ differs from that of MWCNT polarizability. Increase of MWCNT length leads to the increase of both real and imaginary parts of polarizability and also to shift of the maximum of the IM part of the polarizability to the lower frequencies.

The transmission and reflection of composite with corresponding $\varepsilon_{\parallel}$ component are shown in Fig. 7. The amplitude of reflection oscillation is the largest for the shortest nanotubes and gradually decreases with increasing of nanotube length (Fig. 7(b)). The transmission T also decreases with MWCNT length (Fig. 7(a)). Analysis of Fig. 7 shows that composites containing relativity long tubes (length $l \geq 4\,\mu$m) may be potentially used as THz beam polarizer.

We suppose that the length $l = 8\,\mu$m of MWCNT with average outer radius $r = 15$ nm is most suitable for the

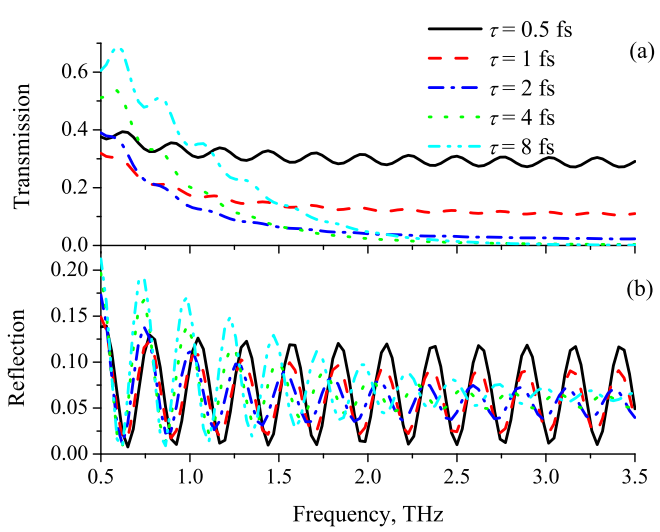

FIG. 5. (a) Transmission and (b) reflection of MWCNT-based composite for different relaxation times. Polarization of incident light is parallel to the nanotube axis. The fitting parameters: $\chi = 1.7$, $l = 1.2\,\mu$m, $r = 15$ nm, $n = 0.5$ wt.%, $\varepsilon_h = 2.5$, $d = 360\,\mu$m.

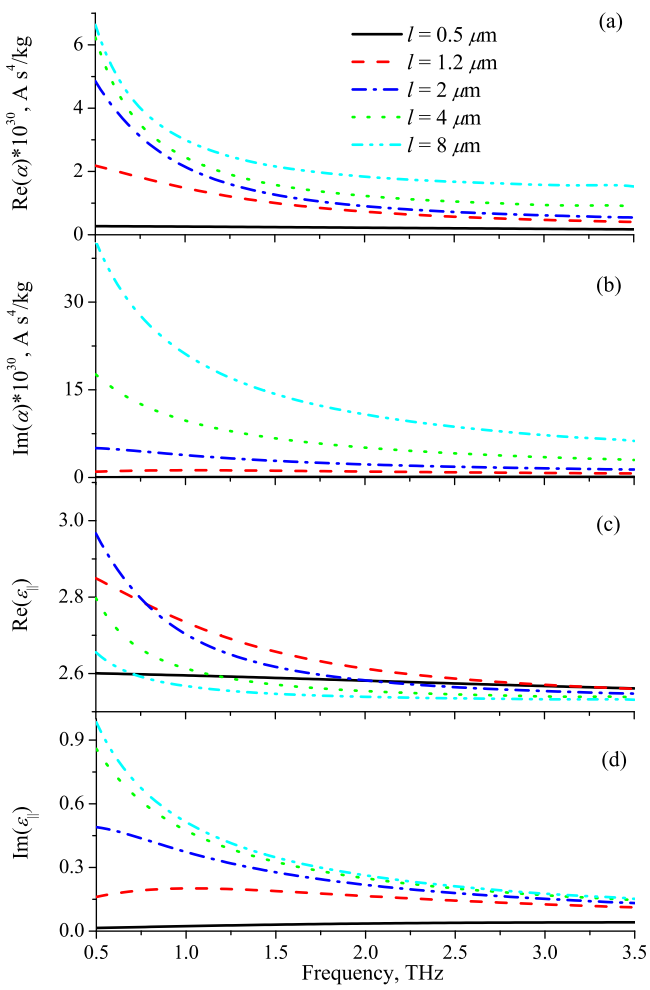

FIG. 6. (a), (b) Frequency dependence of real and imaginary parts of axial polarizability of MWCNT and (c), (d) real and imaginary parts of permittivity $\varepsilon_{\parallel}$ of MWCNT-based composite for various lengths. The fitting parameters: $\chi = 1.7$, $\tau = 2$ fs, $r = 15$ nm, $n = 0.5$ wt.%, $\varepsilon_h = 2.5$.

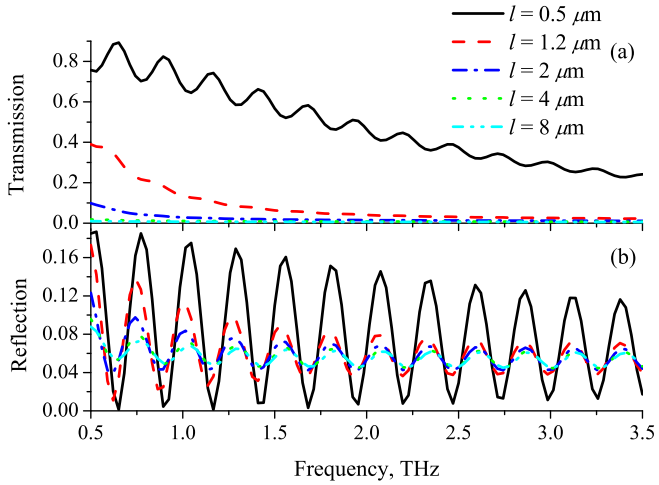

FIG. 7. (a) Transmission and (b) reflection of MWCNT-based composite for various lengths. Polarization of incident wave is parallel to the nanotube axis. The fitting parameters: $\chi = 1.7$, $\tau = 2$ fs, $r = 15$ nm, $n = 0.5$ wt.%, $\varepsilon_h = 2.5$, $d = 360\ \mu$m.

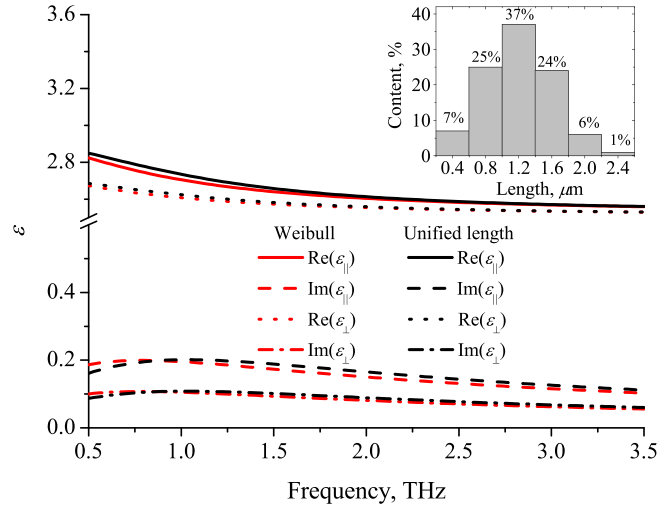

FIG. 8. Frequency dependence of dielectric permittivity of composite containing MWCNTs of unified length $l = 1.2\ \mu$m and composite containing MWCNTs with Weibull length distribution with parameters $l_m = l_a = 1.2\ \mu$m (inset: histogram view of Weibull distribution with parameters $l_m = l_a = 1.2\ \mu$m). The fitting parameters: $\chi = 1.7$, $\tau = 2$ fs, $r = 15$ nm, $n = 0.5$ wt.%, $\varepsilon_h = 2.5$.

THz-polarizer applications. The further increase in the length has no noticeable effect on the electromagnetic response of composite. Actually, although the polarizability of MWCNT with $l > 8\ \mu$m growths when l increases, for constant weight concentration of filler $n = 0.5$ wt. % the number of nanoparticles decreases. Finally for the longer than 8 μm length tubes, being 15 nm in diameter, these two factors compensate each other, and the electromagnetic response in THz range will not be longer dependent on MWCNTs length. We suppose that this will be valid until the MWCNT length is much less than the wavelength of incident radiation. Thus the minimal MWCNT length limit for effective THz-polarizer applications was determined. This is especially important because production of extra long and extra short CNTs currently still remain challenge.

It is worth to point out that Figs. 6 and 7 present ideal case when composite contains MWCNTs of unified length, but in reality there exists a length distribution of the nanotubes which might be modeled by the Weibull probability distribution[30]

$$f(x) = \frac{k}{\lambda}\left(\frac{x}{\lambda}\right)^{k-1} \exp\left(-\left(\frac{x}{\lambda}\right)^{k}\right), \tag{9}$$

where $x \geq 0$, λ is the scale factor, and k is the shape factor. These parameters can be determined from the mode MWCNT length l_m and average MWCNT length l_a in composite, which may be measured experimentally.

Fig. 8 compares the frequency dependence of dielectric permittivity of composite containing MWCNTs with identical length $l = 1.2\ \mu$m and composite with Weibull length MWCNT distribution for parameters $l_m = l_a = 1.2\ \mu$m.

Dielectric permittivity of composite containing MWCNTs with length dispersion may be calculated from (1) replacing the second term in right side by the sum of similar terms with corresponded parameters $N_i, \alpha_{\|i}, n_{\|i}$ for each i-th MWCNT length fraction. We see that accounting of MWCNT length distribution does not affect significantly the electromagnetic response of composite. So Figs. 6 and 7 provide suitable insight into electromagnetic properties of real MWCNT-based composites. We suppose that this result will be useful for practical applications, because control of MWCNT length distribution during composites preparation is currently an intricate problem.

IV. CONCLUSION

Electromagnetic response of polystyrene composites with 0.5 wt. % MWCNT loading prepared by forge rolling method has been experimentally measured and theoretically modeled. Alignment of MWCNTs in polymer matrix causes strong dependence of the transmission/reflection THz spectra on orientation of sample in respect to the electric field, which opens prospects in application of anisotropic MWCNT-based composites for THz polarizers. Best fitting of the experimental data allows defining the structural parameters of the composites such as effective length and electron relaxation time in the nanotubes and their orientation ordering. Simulation shows that the increase of the relaxation time leads to considerable decrease of the transmission at high frequencies and also decrease of amplitude of reflection oscillations. This implies that (i) MWCNTs with minimum amount of defects (for example annealed MWCNTs) are most suitable for THz-radiation absorption, but defective MWCNTs (with $\tau \geq 2$ fs) also may be used for production of effective THz shielding and absorbing composites. Significant decrease of transmission and reflection oscillations is also predicted for MWCNT length up to $\sim 8\ \mu$m, i.e., (ii) minimal MWCNT length limit for effective THz-polarizer applications was determined. (iii) MWCNT length distribution does not affect significantly the electromagnetic response of composite; hence, it may be neglected. Finally we demonstrate that low-cost MWCNT dilute polymer composite gives comparable performance to single-walled CNT-based THz polarizer technologies.[13]

ACKNOWLEDGMENTS

We are grateful to Mr. A. V. Ishchenko for the TEM measurements. The work was financially supported by the RFBR (Grant No. 12-02-90011), EU Projects FP7-266529 BY-NanoERA, PIRSES-2012-318617 FAEMCAR, and PIRSES-GA-2013-610875 NAmiceMC, and BRFBR project FR12-030.

[1]G. Y. Slepyan, S. A. Maksimenko, A. Lakhtakia, O. Yevtushenko, and A. V. Gusakov, "Electrodynamics of carbon nanotubes: Dynamic conductivity, impedance boundary conditions, and surface wave propagation," Phys. Rev. B **60**, 17136–17149 (1999).

[2]K. G. Batrakov, O. V. Kibis, P. P. Kuzhir, M. R. da Costa, and M. E. Portnoi, "Terahertz processes in carbon nanotubes," J. Nanophotonics **4**, 041665 (2010).

[3]S. Nanot, E. H. Hroz, J.-H. Kim, R. H. Hauge, and J. Kono, "Optoelectronic properties of single-wall carbon nanotubes," Adv. Mater. **24**, 4977–4994 (2012).

[4]N. Akima, Y. Iwasa, S. Brown, A. Barbour, J. Cao, J. Musfeldt, H. Matsui, N. Toyota, M. Shiraishi, H. Shimoda, and O. Zhou, "Strong anisotropy in the far-infrared absorption spectra of stretch-aligned single-walled carbon nanotubes," Adv. Mater. **18**, 1166–1169 (2006).

[5]G. Y. Slepyan, M. V. Shuba, S. A. Maksimenko, C. Thomsen, and A. Lakhtakia, "Terahertz conductivity peak in composite materials containing carbon nanotubes: Theory and interpretation of experiment," Phys. Rev. B **81**, 205423-6 (2010).

[6]D. Seliuta, I. Kasalynas, J. Macutkevic, G. Valusis, M. V. Shuba, P. P. Kuzhir, G. Y. Slepyan, S. A. Maksimenko, V. K. Ksenevich, V. Samuilov, and Q. Lu, "Terahertz sensing with carbon nanotube layers coated on silica fibers: Carrier transport versus nanoantenna effects," Appl. Phys. Lett. **97**, 073116-3 (2010).

[7]M. V. Shuba, A. G. Paddubskaya, A. O. Plyushch, P. P. Kuzhir, G. Y. Slepyan, S. A. Maksimenko, V. K. Ksenevich, P. Buka, D. Seliuta, I. Kasalynas, J. Macutkevic, G. Valusis, C. Thomsen, and A. Lakhtakia, "Experimental evidence of localized plasmon resonance in composite materials containing single-wall carbon nanotubes," Phys. Rev. B **85**, 165435-6 (2012).

[8]G. W. Hanson, "Fundamental transmitting properties of carbon nanotube antennas," IEEE Trans. Antennas Propag. **53**, 3426–3435 (2005).

[9]G. Y. Slepyan, M. V. Shuba, S. A. Maksimenko, and A. Lakhtakia, "Theory of optical scattering by achiral carbon nanotubes and their potential as optical nanoantennas," Phys. Rev. B **73**, 195416-11 (2006).

[10]P. J. Burke, S. Li, and Z. Yu, "Quantitative theory of nanowire and nanotube antenna performance," IEEE Trans. Nanotechnol. **5**, 314–334 (2006).

[11]G. Miano and F. Villone, "An integral formulation for the electrodynamics of metallic carbon nanotubes based on a fluid model," IEEE Trans. Antennas Propag. **54**, 2713–2724 (2006).

[12]T.-I. Jeon, K.-J. Kim, C. Kang, S.-J. Oh, J.-H. Son, K. H. An, D. J. Bae, and Y. H. Lee, "Terahertz conductivity of anisotropic single walled carbon nanotube films," Appl. Phys. Lett. **80**, 3403–3405 (2002).

[13]L. Ren, C. L. Pint, T. Arikawa, K. Takeya, I. Kawayama, M. Tonouchi, R. H. Hauge, and J. Kono, "Broadband terahertz polarizers with ideal performance based on aligned carbon nanotube stacks," Nano Lett. **12**, 787–790 (2012).

[14]D. Bychanok, M. Kanygin, A. Okotrub, M. Shuba, A. Paddubskaya, A. Pliushch, P. Kuzhir, and S. Maksimenko, "Anisotropy of the electromagnetic properties of polymer composites based on multiwall carbon nanotubes in the gigahertz frequency range," JETP Lett. **93**, 607–611 (2011).

[15]L. X. Benedict, S. G. Louie, and M. L. Cohen, "Static polarizabilities of single-wall carbon nanotubes," Phys. Rev. B **52**, 8541–8549 (1995).

[16]F. Qin and C. Brosseau, "A review and analysis of microwave absorption in polymer composites filled with carbonaceous particles," J. Appl. Phys. **111**, 061301-24 (2012).

[17]K. Jeon, L. Lumata, T. Tokumoto, E. Steven, J. Brooks, and R. G. Alamo, "Low electrical conductivity threshold and crystalline morphology of single-walled carbon nanotubes high density polyethylene nanocomposites characterized by SEM, Raman spectroscopy and AFM," Polymer **48**, 4751–4764 (2007).

[18]S. Barrau, P. Demont, A. Peigney, C. Laurent, and C. Lacabanne, "Dc and ac conductivity of carbon nanotubes polyepoxy composites," Macromolecules **36**, 5187–5194 (2003).

[19]J. N. Coleman, S. Curran, A. B. Dalton, A. P. Davey, B. McCarthy, W. Blau, and R. C. Barklie, "Percolation-dominated conductivity in a conjugated-polymer-carbon-nanotube composite," Phys. Rev. B **58**, R7492–R7495 (1998).

[20]I. Mazov, V. Kuznetsov, S. Moseenkov, A. Usoltseva, A. Romanenko, O. Anikeeva, T. Buryakov, P. Kuzhir, S. Maksimenko, D. Bychanok, J. Macutkevic, D. Seliuta, G. Valusis, J. Banys, and P. Lambin, "Electromagnetic shielding properties of MWCNT/PMMA composites in Ka-band," Phys. Status Solidi B **246**, 2662–2666 (2009).

[21]A. Okotrub, L. Bulusheva, A. Kudashev, V. Belavin, and S. Komogorcev, "Arrays of carbon nanotubes grown perpendicular to substrate: Anisotropy of structure and properties," Nanotechnol. Russia **3**, 191–200 (2008).

[22]N. Gavrilov, A. Okotrub, L. Bulusheva, O. Sedelnikova, I. Yushina, and V. Kuznetsov, "Dielectric properties of polystyrene/onion-like carbon composites in frequency range of 0.5-500 kHz," Comput. Sci. Technol. **70**, 719–724 (2010).

[23]A. V. Okotrub, V. V. Kubarev, M. A. Kanygin, O. V. Sedelnikova, and L. G. Bulusheva, "Transmission of terahertz radiation by anisotropic MWCNT/polystyrene composite films," Phys. Status Solidi B **248**, 2568–2571 (2011).

[24]A. Priou, *Dielectric Properties of Heterogeneous Materials* (Elsevier Science, Ltd., 1992).

[25]L. Landau and E. Lifshitz, *Electrodynamics of Continuous Media, Course of Theoretical Physics* (Pergamon Press, 1960), Vol. 8.

[26]M. V. Shuba, G. Y. Slepyan, S. A. Maksimenko, C. Thomsen, and A. Lakhtakia, "Theory of multiwall carbon nanotubes as waveguides and antennas in the infrared and the visible regimes," Phys. Rev. B **79**, 155403–155417 (2009).

[27]J. Birch, "The far-infrared optical constants of polypropylene, PTFE and polystyrene," Infrared Phys. **33**, 33–38 (1992).

[28]O. Sedelnikova, N. Gavrilov, L. Bulusheva, and A. Okotrub, "Maxwell-Garnett description of permittivity of onion-like carbon polystyrene composites," J. Nanoelectron. Optoelectron. **4**, 267–270 (2009).

[29]M. Kanygin, O. Sedelnikova, I. Asanov, L. Bulusheva, A. Okotrub, P. Kuzhir, A. Plyushch, S. Maksimenko, K. Lapko, A. Sokol, O. Ivashkevich, and P. Lambin, "Effect of nitrogen doping on the electromagnetic properties of carbon nanotube-based composites," J. Appl. Phys. **113**, 144315-8 (2013).

[30]S.-Y. Fu, Z.-K. Chen, S. Hong, and C. C. Han, "The reduction of carbon nanotube (CNT) length during the manufacture of CNT/polymer composites and a method to simultaneously determine the resulting CNT and interfacial strengths," Carbon **47**, 3192–3200 (2009).